

All crosses were performed by mixing equal volumes of fresh Penassay broth cultures (of the two parental strains) that have about  $5 \times 10^8$  bacteria per milliliter. The mixtures were allowed to stand for 30 minutes at 37°C and then were plated on minimum lactose plates. A total of 3.2 ml of mating mixture was plated for each cross. The plates were incubated at 37°C for 48 hours, and the lac<sup>+</sup> colonies were counted. This method of crossing F<sup>-</sup> with F' lac bacteria gives about ten times more recombinants per plate than were obtainable with crosses between Hfr and F<sup>-</sup> strains. This is critical in these experiments because of the very low recombination rates to be measured. The origin of the lac<sup>-</sup> mutants and the construction of the double mutants have been previously described (4, 5). A map of all the markers used in these experiments is shown in Fig. 1.

To establish the orientation of the nonsense triplets, seven different crosses were performed (Table 1). "Nonrecombinant controls" are those crosses that would be expected to give no recombination. The lac<sup>+</sup> colonies on these controls arise from a mixture of reversion and recombination events, that is, the reversion of one of the two lac<sup>-</sup> markers in a double mutant preceded or followed by a recombination which separates it from the other lac<sup>-</sup> marker. The maximum number of lac<sup>+</sup> colonies in a control was four, as compared to 35 where recombination takes place. It is also clear (Table 1) that the crosses between UGA and UAA and between UAG and UAA fall into the nonrecombinant class, as expected. The UAA mutant was derived in a single step from the UGA mutant (4). The single crossover class exceeds the triple crossover class by fivefold, thus clearly establishing the orientation of the codons as operator ... UAG (or UGA). This is the order generally assumed and is consistent with the tryptophan synthetase results above.

The last line of Table 1 shows the number of colonies observed when the UGA mutant and the nearest outside marker are crossed under identical conditions to the other crosses. The distance between these markers was previously shown to be less than 0.1 percent (6). From these data, the recombination frequency for a single base pair can be calculated to be less than  $3.5 \times 10^{-5}$  percent. The length of the whole  $\beta$ -galactosidase gene is about  $3.3 \times 10^3$  bases, as calculated

from the polypeptide molecular weight (7). Thus, the expected recombination length of the whole Z gene obtained by multiplying the single base-pair recombination frequency by the number of base pairs is about 0.1 percent. The observed value of the length of the Z gene, as measured by ordinary recombination frequency, is about 1 percent; this is ten times larger than expected from the single base-pair recombination frequency.

Recombination between the three nonsense triplets (UGA, UAG, and UAA) mapping in the same codon qualitatively follows the ordinary rules of genetics: recombination is only observed when there are two noncomplementary base pairs in the same codon; that is, the cross between UGA and UAG gives recombination, but the crosses between UGA or UAG and UAA do not. Multiple recombination events are much less frequent than single ones, allowing the ordering of adjacent nucleotide markers.

When the quantitative aspects of adjacent nucleotide recombination are studied, however, the results are more complex. The frequency of recombination between adjacent bases is an order of magnitude too low to account for the total observed recombination length of the  $\beta$ -galactosidase gene. This result is just the opposite of what would be expected from studies of recombination between close markers. As markers get closer together, an increase in the ratio of recombination frequency to distance is observed. This

is hypothesized to be due to enzyme systems which excise regions of hybrid DNA in which there are nucleotide mispairs (8). Such excision and then repair would lead to a much higher frequency of recombination between close markers than expected if an actual break-and-join event had to take place between them.

Our explanation of the low recombination frequency between adjacent nucleotides is that neighboring mispaired nucleotides tend to be excised together from hybrid DNA duplexes. If both markers are removed together, the excision mechanism would not contribute to the recombination frequency. Thus, the recombination frequency would be much lower than expected from studies of markers in which the excision mechanisms make a major contribution to recombination.

DAVID ZIPSER

Department of Biological Sciences,  
Columbia University, New York 10027

#### References

1. J. R. Guest and C. Yanofsky, *Nature* **210**, 799 (1966).
2. Abbreviations: mRNA, messenger RNA; U, uracil; A, adenine; G, guanine; T, thymine; UGA, TGA, UAG, UAA, and UGG, nucleotides.
3. S. Brenner, L. Barnett, E. R. Katz, F. H. C. Crick, *Nature* **213**, 449 (1967).
4. D. Zipser, *J. Mol. Biol.*, in press.
5. ——— and A. W. Newton, *ibid.* **25**, 567 (1967).
6. A. W. Newton, J. Beckwith, D. Zipser, S. Brenner, *ibid.* **14**, 290 (1965).
7. J. L. Brown, S. Koorajian, J. Katze, I. Zabin, *J. Biol. Chem.* **241**, 2826 (1966).
8. R. Holliday, *Genet. Res.* **5**, 282 (1964).
9. Supported in part by NSF grant GB3231 and NIH grant GM14676-01.

19 July 1967

## Hydrous Sodium Silicates from Lake Magadi, Kenya: Precursors of Bedded Chert

**Abstract.** *Two new hydrous sodium silicates,  $\text{NaSi}_7\text{O}_{13}(\text{OH})_3 \cdot 3\text{H}_2\text{O}$  (magadiite) and  $\text{NaSi}_{11}\text{O}_{20.5}(\text{OH})_4 \cdot 3\text{H}_2\text{O}$  (kenyaite), were found in lake beds at Lake Magadi, Kenya. Both are well-crystallized layered silicates with large basal spacings. Concretions within the magadiite bed consist of kenyaite or quartz (chert) in the center, surrounded by kenyaite. In dilute acids magadiite and kenyaite are converted to  $6\text{SiO}_2 \cdot \text{H}_2\text{O}$  (SH), the first known crystalline hydrate of silica. The magadiite bed probably represents a chemical precipitate from alkaline brines. Percolating waters convert magadiite to kenyaite and eventually to chert. Thus a mechanism has been outlined for the formation of bedded chert deposits through inorganic precipitation. Alternations between silica-rich and iron-rich bands of iron formations may be due to concentration cycles in alkaline lakes.*

The Eastern, or Gregory Rift Valley, in East Africa contains a number of sodium carbonate-rich, alkaline lakes (1); the most saline of these is Lake Magadi in southern Kenya (2). It lies in a closed basin at 1978 feet

(603 m) above sea level in the heavily block-faulted floor of the valley, 2° south of the equator. It is intermittently dry, except for brine pools ("lagoons") near the margins. It contains a vast deposit of trona ( $\text{Na}_2\text{CO}_3 \cdot \text{NaHCO}_3$

Table 1. Chemical analyses of magadiite, kenyaite, and SH, percentage by weight. The analyst was O. Von Knorring. SH was prepared from magadiite + 1/10N HCl. Magadiite reconstituted was prepared from SH + 1M Na<sub>2</sub>CO<sub>3</sub>. Approximate formula: magadiite, NaSi<sub>7</sub>O<sub>13</sub>(OH)<sub>8</sub> · 3H<sub>2</sub>O, kenyaite, NaSi<sub>11</sub>O<sub>20.5</sub>(OH)<sub>4</sub> · 3H<sub>2</sub>O; SH, 6SiO<sub>2</sub> · H<sub>2</sub>O, or H<sub>2</sub>Si<sub>6</sub>O<sub>13</sub>.

Chemical	Magadiite	Kenyaite	SH	Magadiite reconstituted
SiO <sub>2</sub>	77.62	83.50	92.70	78.79
TiO <sub>2</sub>	0.06	0.02	0.04	0.03
Al <sub>2</sub> O <sub>3</sub>	.79	.22	.52	.50
Fe <sub>2</sub> O <sub>3</sub>	.55	.09	.34	.12
MnO	.01	trace	<.01	<.01
MgO	.26	0.04	.10	.05
CaO	.14	.11	.16	.14
Na <sub>2</sub> O	5.55	3.96	.20	5.55
K <sub>2</sub> O	0.35	0.04	.22	0.16
H <sub>2</sub> O+	5.28	4.90	4.74	5.20
H <sub>2</sub> O-	9.32	7.10	0.86	9.65
		<i>Mole fractions</i>		
Na <sub>2</sub> O	1.000	1.000	0.012	1.000
SiO <sub>2</sub>	14.432	21.746	6.000	14.650
H <sub>2</sub> O+	3.275	4.257	1.023	3.225
H <sub>2</sub> O-	5.780	6.167	0.186	5.984

2H<sub>2</sub>O), which has been mined for a number of years. It is fed by several groups of hot springs and by seasonal runoff. The hills surrounding Lake Magadi are formed by Pleistocene alkali trachyte flows and the valleys by a series of lake beds dating from the Middle Pleistocene to Recent. The shoreline of a high stage of Lake Magadi, some 40 feet (12 m) above the present level, is clearly discernible in many places. The High Magadi beds (2) of Upper Pleistocene to Recent age were deposited from this more dilute precursor of Lake Magadi. They consist of up to 10 feet (3 m) of well-bedded green and brown clays and silts, a thin bed crowded with black fish skeletons, identified as *Tilapia Nilotica* (2), followed by 20 to 30 feet (6.1 to 9.2 m) of faintly laminated brown silts. The High Magadi beds rest unconformably either on the trachyte lavas or on the Chert Series rocks. Baker (2, pp.

37-40) has illustrated several sections through these beds. In one he noted:

... a thin horizon of white slightly plastic powder about one and a half inches thick. . . this material proved to be extremely finely divided silica devoid of organic structure which, on the drying out of some specimens, became hard and porcellaneous. It is concluded that the bed represents a chemical precipitate of colloidal silica which has not yet been converted to chert by recrystallization.

During a recent study of the geochemistry and mineralogy of Lake Magadi, this white layer was found to be present in all High Magadi sections, varying in thickness from a few inches to 2 feet (0.6 m). It appears immediately below the *Tilapia* bed and can be used as a stratigraphic marker. Its maximum thickness was encountered in the valley floor, east of the town of Magadi, where it lies below at least 6 feet (1.8 m) of the hard, faintly laminated brown silts (Fig. 1). In the remnants of the

High Magadi beds toward the periphery of the basin, it thins considerably and splits into a number of smaller layers, some less than 1 inch thick (Fig. 2). It is always finely laminated, with dark impurities (mainly clay minerals) marking the laminae, which are roughly 1 mm thick. This white layer, with the consistency of soft putty, is composed predominantly of spherulites of a well-crystallized hydrous sodium silicate, here named magadiite. It also contains a small amount of well crystallized rosettes of calcite. In some magadiite beds a number of hard nodular concretions were found, which consist of another well crystallized hydrous sodium silicate, here named kenyaite. Some of the larger concretions have a core of hard, laminated chert consisting of quartz. Magadiite and kenyaite have an average refractive index of 1.48.

When either magadiite or kenyaite is treated with dilute acid (including unbuffered EDTA) at room temperature, they are converted to a hydrous phase of silica, here identified as SH. This phase was not encountered in the natural deposits. It is the first known crystalline hydrate of silica.

Chemical compositions of magadiite, kenyaite, and SH are given in Table 1. The minerals were prepared for analysis by repeated washing in water to remove all traces of the pore brine which contains NaCl, NaHCO<sub>3</sub>, and Na<sub>2</sub>CO<sub>3</sub>. They were then treated with buffered EDTA to remove the disseminated calcite, and dried at 110°C. When SH, prepared from magadiite, is stirred at 25°C in concentrated solutions of either NaOH or Na<sub>2</sub>CO<sub>3</sub>, it is reconverted to magadiite. An analysis of this reconstituted magadiite is also given in Table 1.

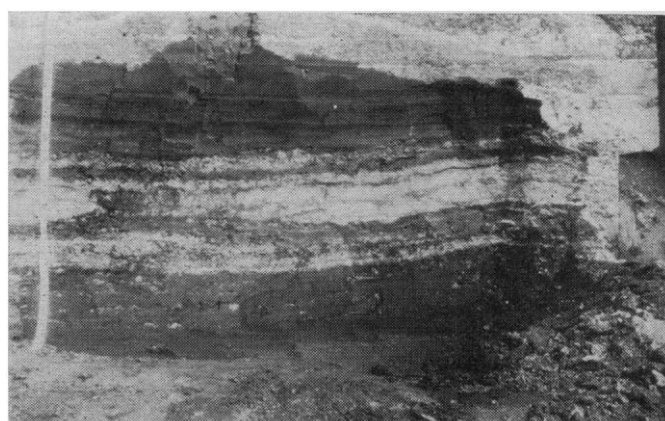


Fig. 1. Laminated magadiite bed (white), exposed in a pit about 2 feet below brown silts in the floor of the alluvial channel east of the town of Magadi and south of the road. Scale in inches. The black *Tilapia* bed may be seen 3 inches above the top of the magadiite bed. Fig. 2. Laminated magadiite beds (white) in an outcrop of High Magadi beds near the mouth of Olkeju Ekisichiyo, east of Magadi. Scale in inches. The *Tilapia* bed again appears as a black layer 3 inches above the highest magadiite bed.

In a similar manner, SH prepared from kenyaite can be reconverted to kenyaite, indicating some structural inheritance.

Table 1 shows that magadiite and kenyaite are relatively free of impurities and consist essentially of sodium, silicon, and water, whereas SH is essentially pure silica hydrate. The reconstituted magadiite, made from SH + Na<sub>2</sub>CO<sub>3</sub>, is surprisingly close to the original material in composition, except that impurities decreased somewhat during the treatment. This seems to indicate that not only Na, but also H<sub>2</sub>O+ and even H<sub>2</sub>O- occupy fixed sites in

Table 2. X-ray diffraction pattern of magadiite, measured with quartz as internal standard. Indexed assuming tetragonal symmetry. *I*, arbitrary intensity scale; *d<sub>calc</sub>*, calculated from the refined cell dimensions given in Table 5. The following three weak peaks have been assigned to a chlorite-type impurity: *d* = 7.213 Å, *I* = 3, *hkl* = 002; *d* = 4.699 Å, *I* = 3, *hkl* = 003; *d* = 3.632 Å, *I* = 10, *hkl* = 004. An additional peak at *d* = 6.860, *I* = 3 probably also belongs to a similar layered silicate.

<i>I</i>	<i>d<sub>obs</sub></i>	<i>d<sub>calc</sub></i>	<i>hkl</i>
100	15.41	15.57	001
9	7.755	7.786	002*
		7.743	111
4	5.612	5.644	210*
19	5.181	5.191	003*
16	5.007	4.902	202
18	4.464	4.487	113
		4.462	220*
9	4.008	4.009	203
		3.991	130
4	3.909	3.893	004
12	3.543	3.551	312*
80	3.435	3.415	321*
35	3.296	3.270	303
10	3.200	3.205	214
50	3.146	3.155	400*
3	2.994	3.003	411
		2.975	330
3.5	2.864	2.857	304
2.5	2.818	2.822	420*
3.5	2.721	2.727	215
5	2.642	2.637	413*
4.5	2.592	2.596	006
		2.581	333
3.5	2.520	2.524	500, 430
2	2.396	2.401	206, 432, 502
4.5	2.352	2.344	520
2.5	2.259	2.270	433
		2.244	226, 522
1	2.161	2.159	117
2.5	2.060	2.057	611
4	1.992	1.991	227
1	1.940	1.943	317
		1.938	515
1	1.869	1.868	631
1	1.777	1.777	535
		1.776	624
1	1.737	1.739	641
		1.734	720
1	1.667	1.666	545
1.5	1.638	1.636	704
1.5	1.562	1.560	705
2	1.491	1.492	654

\* Reflections used in the least-square refinement (4); cell dimensions given in Table 5.

the lattice. Arbitrarily assigning the H<sub>2</sub>O+ (> 110°C) to (OH) groups, the H<sub>2</sub>O- to (H<sub>2</sub>O), and simplifying the atomic ratios somewhat, we can express the composition of magadiite as NaSi<sub>7</sub>O<sub>13</sub>(OH)<sub>3</sub>·3 H<sub>2</sub>O and that of kenyaite as NaSi<sub>11</sub>O<sub>20.5</sub>(OH)<sub>4</sub>·3H<sub>2</sub>O. The composition of SH is 6SiO<sub>2</sub>·H<sub>2</sub>O or H<sub>2</sub>Si<sub>6</sub>O<sub>13</sub>. The exact atomic ratios are somewhat uncertain because of clay-type impurities (Tables 2-4) present, the difficulty of removing all the adsorbed sodium, and because of the use of the traditional 110°C separation for H<sub>2</sub>O+ and H<sub>2</sub>O-, which may not be applicable in this case.

Table 1 shows that when magadiite is acidified (*pH* < 5), virtually all of its sodium and most of the H<sub>2</sub>O- is removed during the conversion to SH. Both of these constituents are restored to their original levels during reconstitution in sodium-rich solutions. K<sup>+</sup> and NH<sub>4</sub><sup>+</sup> can be substituted for Na<sup>+</sup> but the products show considerably different x-ray patterns.

The x-ray diffraction patterns of magadiite, kenyaite, and SH are given in Tables 2 to 4. All three phases are extremely fine-grained and single crystals are not available. However, powder patterns are very characteristic. All obviously belong to layered structures with very large basal spacings (15.4, 19.7, and 13.6 Å, respectively). They are easy to distinguish, though a number of similarities exist, particularly between those of magadiite and kenyaite. A certain resemblance was noted with the pattern of keatite, or SiO<sub>2</sub>-K (3), which also has a strong reflection near 3.43 Å. For this reason, the three new phases were indexed on tetragonal cells, with the *a* dimension arrived at by trial and error. Tetragonal cells fit all three phases reasonably well, though this is no proof that they do not in fact crystallize in a system of lower symmetry. Cell dimensions were refined using a least squares computer program (4). The results are given in Table 5. No obvious relations exist between cell dimensions and compositions. The ease with which magadiite and kenyaite can be converted to SH and vice versa suggests that a basic structural similarity exists. The SiO<sub>2</sub>:H<sub>2</sub>O ratio of SH depends on the water determination. Though repeated determinations gave similar results, it is tempting to speculate that all three structures are built up of sheets of SiO<sub>4</sub> tetrahedra, with 7SiO<sub>2</sub> per sheet and that the sheets are linked by NaOH and H<sub>2</sub>O in magadiite and kenyaite and

by H<sub>2</sub>O in SH. Jamieson (5) found a sheet structure for Na<sub>2</sub>Si<sub>3</sub>O<sub>7</sub>.

Attempts at synthesis of magadiite and kenyaite and at conversion of one to the other have been unsuccessful. Recrystallization under pressure above 100°C yields quartz and heating to 700°C in air produces tridymite + quartz. Heating in air at 110° for many

Table 3. X-ray diffraction pattern of kenyaite. Measured with quartz and silicon as internal standards. Indexed assuming tetragonal symmetry. Abbreviations same as in Table 2. A small peak at *d* = 7.272 Å, *I* = 5 probably belongs to a kaolinite or chlorite-type impurity (see Table 2). The peak at *d* = 5.142, *I* = 12 cannot be indexed on a tetragonal cell and may also belong to an impurity.

<i>I</i>	<i>d<sub>obs</sub></i>	<i>d<sub>calc</sub></i>	<i>hkl</i>
100	19.68	19.87	001
50	9.925	9.937	002*
2	7.775	7.852	102
5	6.620	6.625	003
7	5.637	5.729	210
		5.505	211
12	5.142		
35	4.965	4.969	004
		4.963	212
28	4.689	4.633	104*
5	4.471	4.529	220
10	3.945	3.969	131
		3.926	204
5	3.754	3.754	214
		3.751	312
20	3.638	3.640	115*
22	3.525	3.497	321*
85	3.428	3.456	313*
45	3.320	3.313	006
55	3.198	3.202	400*
14	2.934	2.942	206*
12	2.827	2.835	421
		2.813	413
3	2.652	2.747	333
3	2.520	2.512	510
3	2.480	2.482	424
		2.481	502, 432
5	2.416	2.423	326
7	2.343	2.349	513
3	1.880	1.881	605, 517

\* Reflections used in the least-square refinement (4); cell dimensions given in Table 5.

Table 4. X-ray diffraction pattern of the synthetic phase SH, measured with quartz as internal standard. Indexed assuming tetragonal symmetry. Abbreviations same as in Table 2. A peak at *d* = 7.326 Å, *I* = 35, was assigned to a kaolinite or chlorite-type impurity. SH prepared from magadiite + 1/10N HCl, 25°C.

<i>I</i>	<i>d<sub>obs</sub></i>	<i>d<sub>calc</sub></i>	<i>hkl</i>
100	13.61	13.68	001*
45	6.862	6.839	002*
12	6.134	6.053	102
25	4.699	4.711	202*
35	4.122	4.131	301*
		4.111	310
30	3.664	3.660	302*
30	3.572	3.588	213*
75	3.428	3.420	004*
10	3.261	3.250	400

\* Reflections used in the least-square refinement (4); cell dimensions given in Table 5.

Table 5. Cell dimensions of magadiite, kenyaite, SH, and keatite, assuming tetragonal symmetry.

Dimensions	Magadiite*	Kenyaite*	SH*	Keatite†
a, Å	12.620 ± 0.020	12.810 ± 0.054	13.000 ± 0.032	7.456
c, Å	15.573 ± 0.079	19.875 ± 0.094	13.678 ± 0.029	8.604
V, Å <sup>3</sup>	2480.2 ± 12.81	3261.5 ± 27.49	2311.4 ± 10.73	478.3

\* Data from Tables 2-4. † Data from Shropshire *et al.* (3).

months does not change the x-ray pattern of either mineral. Hence the H<sub>2</sub>O from H<sub>2</sub>O— must not occupy structurally sensitive positions. Baker *et al.* (6) in their study of the system Na<sub>2</sub>O — SiO<sub>2</sub> — H<sub>2</sub>O synthesized the compound 3Na<sub>2</sub>O · 13SiO<sub>2</sub> · 11H<sub>2</sub>O, but they did not investigate the compositional range in which magadiite and kenyaite occur.

The geologic implications of the magadiite deposit at Lake Magadi are considerable. Because of its chemical composition and its stratigraphic persistence, (it probably covers over 50 square miles—or 130 km<sup>2</sup>), the magadiite layer most likely represents a chemical precipitate from alkaline brines of the precursor of Lake Magadi. Jones *et al.* (7) found that present-day Magadi brines contain as much as 1450 parts per million SiO<sub>2</sub>. Dilution of such brines by fresh water could precipitate magadiite and the fine lamination may represent annual increments of deposition. During subsequent burial, magadiite remains stable, particularly in the presence of alkaline pore fluids. The formation of kenyaite nodules in the magadiite bed is probably due to a gradual removal of sodium by percolating waters. The presence of laminated chert in the center of the larger nodules indicates that this process continues and may eventually lead to the complete conversion of the magadiite bed to kenyaite and then to a chert bed, still preserving the laminations of the original deposit. SH is not formed in the process because of the high pH values involved. I have outlined a mechanism for the formation of laminated chert deposits in the absence of organic activity. Govett (8) has recently summarized evidence with respect to the depositional environment of the Precambrian iron formations and has concluded that a lacustrine environment is most probable. The mechanism proposed here for the formation of the chert beds can be extended to include the iron-rich bands. In sodium carbonate lakes silica would be precipitated and iron would be stored in solution during the lower-pH, dilute

stage, whereas iron would be precipitated and silica stored in the brines during the dryer, high-pH stages. The alternation would then simply be governed by rainfall and evaporation. We do not yet fully understand why alkaline lakes form (9), but we know that the Na/Ca, CO<sub>2</sub>/Cl, and CO<sub>2</sub>/SO<sub>4</sub> ratios of the inflow waters must be comparatively high. If sodium carbonate species are the main constituents in the closed-basin waters, evaporative concentration will cause a rise in pH well above 9 and as high as 11 (7). Volcanic and igneous terranes are the most obvious sources for such inflow waters, and in fact most alkaline lakes, including Lake Magadi, lie in volcanic terranes. Extensive volcanic terranes were probably much more abundant during Precambrian times, and we may postulate that many lacustrine basins then were of the sodium-carbonate-bicarbonate rather than the sodium-chloride type. This provides a simple explanation for the great preponderance of banded iron formations during the Precambrian.

HANS P. EUGSTER

Department of Geology,  
Johns Hopkins University,  
Baltimore, Maryland 21218

#### References and Notes

- J. F. Talling and I. B. Talling, *Int. Rev. Ges. Hydrobiol.* **50**, 421 (1965).
- B. H. Baker, *Geol. Survey of Kenya* **42** (1958).
- P. P. Keat, *Science* **120**, 328 (1954); J. Shropshire, P. P. Keat, P. A. Vaughan, *Z. Krist.* **112**, 409 (1959).
- C. W. Burnham, in *Carnegie Institution of Washington Year Book 1961* (Carnegie Institution, Washington, D.C., 1962), p. 132.
- P. B. Jamieson, *Nature* **214**, 796 (1967).
- C. L. Baker, L. R. Jue, J. H. Wills, *J. Amer. Chem. Soc.* **72**, 5369 (1950).
- B. F. Jones, S. Rettig, H. P. Eugster, in preparation.
- G. J. S. Govett, *Bull. Geol. Soc. Amer.* **77**, 1191 (1966).
- B. F. Jones, 2nd Northern Ohio Geological Society Symposium on Salt, Cleveland (1966), p. 181.
- Fieldwork supported by a grant from the Petroleum Research Fund. Permission to work at Magadi and generous logistic support by the Magadi Soda Company through W. Rouse, General Manager, is gratefully acknowledged. B. F. Jones read the manuscript and provided access to unpublished data and help with both field and laboratory problems. O. P. Bricker, III, made valuable suggestions and read the manuscript.

5 July 1967

## Lysosomal Enzyme Inhibition by Trypan Blue: A Theory of Teratogenesis

**Abstract.** *A mechanism of mammalian teratogenesis involving inhibition of embryotrophic nutrition is suggested and exemplified by the action of trypan blue on pregnant rats. There is evidence for the localization of trypan blue in heterolysosomes of the epithelium of the visceral yolk sac, and our experiments indicate that the dye is an inhibitor of a selection of hydrolytic enzymes present in lysosomal fractions from homogenates of rat visceral yolk sac. It seems likely that trypan blue inhibits the intracellular digestion of embryotroph by the visceral yolk-sac epithelium; the conceptus may therefore be deprived of essential nutrients at critical stages of development.*

Agents which cause congenital malformations in mammalia must owe their activity to an effect upon the embryo, the mother, or the site of exchange between mother and fetus. Investigations of teratogenic mechanisms must therefore be concerned with the identification of both the target organ and the particular injury which it receives. For the majority of teratogens neither of these problems has been resolved, and in some cases the possibility that drug metabolism takes place renders the identity of the active material uncertain.

Certain features of the teratogenic activity of trypan blue and related bisazo dyes suggest that in rodents the site of their action is the visceral yolk-sac endoderm. Of the available evidence, reviewed elsewhere (1), the following relevant observations may be cited. Action of trypan blue on the embryo seems unlikely since there is no evidence to suggest that the dye is metabolized and since most authors agree that it cannot be demonstrated in embryonic tissues after administration of a teratogenic dose to the mother (2). An indirect action of the dye, mediated by changes in maternal metabolism, is rendered less plausible by the well-documented teratogenic effect of these dyes on chick eggs (3, 4). The yolk-sac endoderm in rodents and chicks actively accumulates trypan blue in large quantities and is the only fetal membrane which does so (5, 6). In the rat, cessation of the teratogenic effect of trypan blue (7) coincides with the es-